Electronic Supplementary Material (ESI) for Dalton Transactions.
This journal is © The Royal Society of Chemistry 2019

Chiral luminescent lanthanide complexes possessing strong (samarium, Sm^{III}) circularly polarised luminescence (CPL), and their self-assembly into Langmuir-Blodgett films

Dawn E. Barry,[a] Jonathan A. Kitchen,*[b] Laszlo Mercs,[c] Robert D. Peacock,[d] Martin Albrecht,[c] and Thorfinnur Gunnlaugsson*[a]*

[a]*School of Chemistry and Trinity Biomedical Science Institute, Trinity College Dublin, Dublin 2, Ireland*.

[b] *Chemistry, School of Natural and Computational Sciences, Massey University, Albany, Auckland, New Zealand.*

[c] *School of Chemistry and Chemical Biology, University College Dublin, Belfield, Dublin 4, Ireland.*

[d]*School of Chemistry, University of Glasgow Glasgow, G12 8QQ, Scotland (UK).*

gunnlaut@tcd.ie,

Supporting Information

General Experimental Details

Complexation reactions were carried out in 2-5 mL Biotage Microwave Vials in a Biotage Initiator Eight EXP microwave reactor. Reactions were performed at 70 ^{o}C for 10 mins in HPLC grade CH_3OH. Elemental analyses were carried out at the Microanalytical Laboratory, School of Chemistry and Chemical Biology, University College Dublin. Infrared spectra were recorded on a Perkin Elmer Spectrum One FT-IR spectrometer equipped with a Universal ATR sampling accessory; solid samples were recorded directly as neat samples in cm^{-1}. Using a 1.0 cm path length quartz cell, UV-visible absorption and luminescence spectra were recorded at room temperature using a Varian CARY 50 spectrophotometer. The solvents employed were of HPLC or spectrophotometric grade. For UV-visible absorption measurements a scan rate of 600 nm min^{-1} was employed and the blank used was a sample of the solvent system in which the titration was undertaken. All absorbance and luminescence scans were measured in arbitrary units. Langmuir measurements were carried out at 25 °C on a KSV MiniMicro Langmuir-Blodgett trough (KSV, Finland). Water was purified with a Milli-Q ® Integral system (Millipore), and its resistivity was measured to be higher than 18 MΩ cm. A 9:1 mixture of CH_3Cl/CH_3OH was used as a spreading solvent and typically drops (20 µL) of the surfactant solution (~0.25 mM) were deposited using a microsyringe on the water subphase. The solvent was left to evaporate for 20 min before the barriers were compressed at 6 mm min^{-1}. Surface pressure was monitored using a platinum Wilhelmy plate. Circular dichroism (CD) spectra were recorded on a Jasco J-810-150S spectropolarimeter in a 1.2 mL cell. Each CD trace represents an average of three scans. All CD are represented as mdeg *vs* λ (nm). Circularly polarised luminescence (CPL) spectra were recorded by Dr. R. Peacock at the University of Glasgow. Excitation was accomplished by using a Coherent 599 tuneable dye laser (0.03 nm resolution) with argon ion laser as a pump source. Calibration of the emission monochromator was accomplished by passing scattered light from a low power HeNe laser through the detection system. The optical detection system consisted of a photoelastic modulator (PEM, Hinds Int.) operating at 50 kHz and a linear polariser, which together act as a circular analyser, followed by a long pass filter, focusing lens and a 0.22 m double monochromator. The emitted light was detected by a cooled EM1-9558QB photomultiplier tube operating in photon counting mode. The 50 KHz reference signal from the photoelastic modulator was used to direct the incoming pulses into two separated counters. An up counter, which counts every photon pulse and thus is a measure of the total luminescence signal $I = I_{left} + I_{right}$, and an up/down counter, which adds pulses when the analyser is transmitting to the left circularly polarised light and subtracts pulses when the analyser is transmitting right circularly polarised light. The second counter provides a measure of the differential emission intensity $\Delta I = I_{left} - I_{right}$.

Experimental details for complexes Ln.**L**$_3$ (Ln = Tb^{III}, Sm^{III}, Lu^{III}, Dy^{III}, **L** = **1** (*R*) or **2** (*S*))

*Synthesis of Tb.**1**$_3$:*

Ligand **1** (0.028 g, 0.05 mmol, 3 equiv.) in 5 mL CH_3OH had solid $Tb(CF_3SO_3)_3$ (0.01 g, 0.02 mmol, 1 equiv.) added and was heated at 70 °C under microwave irradiation for 10 minutes. The resulting clear yellow solution was subjected to vapour diffusion of diethyl ether affording Tb.**1**$_3$ as a white solid in 71% yield. HRMS (*m/z*) (MS-LD$^+$) Calculated for $C_{72}H_{98}F_6N_6O_{10}S_2Tb^+$ *m/z* = 1543.5944. Found *m/z* = 1543.5914; Elemental analysis for $C_{108}H_{147}N_9O_{15}F_9S_3Tb.3H_2O$ (2291.55 gmol^{-1}) Calculated: C 56.61, H 6.73, N 5.50. Found C 56.47, H 6.23, N 5.39%. IR(neat): 3276, 2925, 2854, 1634, 1596, 1558, 1460, 1276, 1198, 1163, 1030, 839, 801, 779, 721 cm^{-1}.

*Synthesis of Sm.**1**$_3$:*

Ligand **1** (0.025 g, 0.05 mmol, 3 equiv.) in 5 mL CH_3OH had solid $Sm(CF_3SO_3)_3$ (0.009 g, 0.02 mmol, 1 equiv.) added and was heated at 70 °C under microwave irradiation for 10 minutes. The resulting clear yellow solution was subjected to vapour diffusion of diethyl ether affording Sm.**1**$_3$ as a white solid in 50% yield. HRMS (*m/z*) (MS-LD$^+$) Calculated for $C_{72}H_{98}F_6N_6O_{10}S_2Sm^+$ *m/z* = 1536.5887. Found *m/z* = 1536.5853; [Elemental analysis for $C_{108}H_{147}N_9O_{15}F_9S_3Sm.$ (2228.925 gmol^{-1}) Calculated: C 58.14, H 6.65, N 5.65. Found C 58.79, H 6.95, N 5.55%. IR(neat): 3283, 2925, 2854, 1633, 1595, 1559, 1458, 1238, 1225, 1165, 1030, 839, 800, 778, 722 cm^{-1}.

*Synthesis of Lu.**1**$_3$:*

Ligand **1** (0.027 g, 0.05 mmol, 3 equiv.) in 5 mL CH_3OH had solid $Lu(CF_3SO_3)_3$ (0.009 g, 0.02 mmol, 1 equiv.) added and was heated at 70 °C under microwave irradiation for 10 minutes. The resulting clear yellow solution was subjected to vapour diffusion of diethyl ether affording Lu.**1**$_3$ as a white solid in 52% yield. HRMS (*m/z*) (MS-LD$^+$) Calculated for $C_{72}H_{98}F_6N_6O_{10}S_2Lu^+$ *m/z* = 1559.6098. Found *m/z* = 1559.5941; [Elemental analysis for $C_{108}H_{147}N_9O_{15}F_9S_3Lu.2H_2O$ (2251.94 gmol^{-1}) Calculated: C 56.64, H 6.65, N 5.50. Found C 56.38, H 6.21, N 5.41%. IR(neat): 3270, 2926, 2854, 1635, 1598, 1562, 1461, 1240, 1161, 1029, 917, 841, 800, 777, 723 cm^{-1}.

*Synthesis of Dy.**1**$_3$:*

Ligand **1** (0.025 g, 0.05 mmol, 3 equiv.) in 5 mL CH_3OH had solid $Dy(CF_3SO_3)_3$ (0.009 g, 0.02 mmol, 1 equiv.) added and was heated at 70 °C under microwave irradiation for 10 minutes. The resulting clear yellow solution was subjected to vapour diffusion of diethyl ether affording Dy.**1**$_3$ as a white solid in 50 % yield. HRMS (*m/z*) (MS-LD$^+$) Calculated for $C_{72}H_{98}F_6N_6O_{10}S_2Dy^+$ *m/z* = 1548.5982. Found *m/z* = 1548.6006; [Elemental analysis for $C_{108}H_{147}N_9O_{15}F_9S_3Dy.3H_2O$ (2240.93 gmol^{-1}) Calculated: C 56.47, H 6.71, N 5.49. Found C 56.08, H 6.53, N 5.35%. IR(neat): 3275, 2925, 2854, 1634, 1596, 1562, 1460, 1240, 1163, 1030, 840, 800, 778, 755, 722 cm^{-1}.

*Synthesis of Tb.**2**$_3$:*

Ligand **2** (0.021 g, 0.04 mmol, 3 equiv.) in 5 mL CH_3OH had solid $Tb(CF_3SO_3)_3$ (0.008 g, 0.01 mmol, 1 equiv.) added and was heated at 70 °C under microwave irradiation for 10 minutes. The resulting clear yellow solution was subjected to vapour diffusion of diethyl ether affording Tb.$\mathbf{2}_3$ as a white solid in 52% yield. HRMS (*m/z*) (MS-LD$^+$) Calculated for $C_{72}H_{98}F_6N_6O_{10}S_2Tb^+$ *m/z* = 1543.5944. Found *m/z* = 1543.5908; Elemental analysis for $C_{108}H_{147}N_9O_{15}F_9S_3Tb.5H_2O$ (2327.56 gmol^{-1}) Calculated: C 55.73, H 6.80, N 5.42. Found C 55.73, H 6.80, N 5.42%. IR(neat): 3282, 2925, 2854, 1634, 1596, 1558, 1457, 1240, 1197, 1164, 1030, 839, 801, 779, 752, 721 cm^{-1}.

*Synthesis of Sm.**2**$_3$:*

Ligand **2** (0.030 g, 0.05 mmol, 3 equiv.) in 5 mL CH_3OH had solid $Sm(CF_3SO_3)_3$ (0.011 g, 0.02 mmol, 1 equiv.) added and was heated at 70 °C under microwave irradiation for 10 minutes. The resulting clear yellow solution was subjected to vapour diffusion of diethyl ether affording Sm.$\mathbf{2}_3$ as a white solid in 46% yield. HRMS (*m/z*) (MS-LD$^+$) Calculated for $C_{72}H_{98}F_6N_6O_{10}S_2Sm^+$ *m/z* = 1536.5887. Found *m/z* = 1536.5863; [Elemental analysis for $C_{108}H_{147}N_9O_{15}F_9S_3Sm.H_2O$ (2246.95 gmol^{-1}) Calculated: C 57.73, H 6.68, N 5.61. Found C 57.45, H 6.40, N 5.83%. IR(neat): 3282, 2925, 2854, 1633, 1595, 1558, 1457, 1238, 1163, 1030, 838, 801, 779, 750 cm^{-1}.

*Synthesis of Lu.**2**$_3$:*

Ligand **2** (0.034 g, 0.06 mmol, 3 equiv.) in 5 mL CH_3OH had solid $Lu(CF_3SO_3)_3$ (0.013 g, 0.02 mmol, 1 equiv.) added and was heated at 70 °C under microwave irradiation for 10 minutes. The resulting clear yellow solution was subjected to vapour diffusion of diethyl ether affording Lu.$\mathbf{2}_3$ as a white solid in 53% yield. HRMS (*m/z*) (MS-LD$^+$) Calculated for $C_{72}H_{98}F_6N_6O_{10}S_2Lu^+$ *m/z* = 1559.6098. Found *m/z* = 1559.6055; [Elemental analysis for $C_{108}H_{147}N_9O_{15}F_9S_3Lu.3H_2O$ (2307.59 gmol^{-1}) Calculated: C 56.21, H 6.68, N 5.58. Found C 56.21, H 5.94, N 5.83%. IR(neat): 3277, 2925, 2854, 1638, 1598, 1561, 1461, 1240, 1199, 1163, 1030, 839, 801, 779, 757, 722 cm^{-1}.

*Synthesis of Dy.**2**$_3$:*

Ligand **2**(0.032 g, 0.06 mmol, 3 equiv.) in 5 mL CH_3OH had solid $Dy(CF_3SO_3)_3$ (0.018 g, 0.03 mmol, 1 equiv.) added and was heated at 70 °C under microwave irradiation for 10 minutes. The resulting clear yellow solutions was subjected to vapour diffusion of diethyl ether affording Dy.$\mathbf{2}_3$ as a white solid in 36 % yield. HRMS (*m/z*) (MS-LD$^+$) Calculated for $C_{72}H_{98}F_6N_6O_{10}S_2Dy^+$ *m/z* = 1548.5982. Found *m/z* = 1548.5920; [Elemental analysis for $C_{108}H_{147}N_9O_{15}F_9S_3Dy.5H_2O$ (2331.13 gmol^{-1}) Calculated: C 55.64, H 6.79, N 5.41. Found C 55.68, H 6.26, N 5.27%. IR(neat): 3277, 2925, 2854, 1635, 1596, 1562, 1460, 1240, 1164, 1030, 840, 800, 778, 755 cm^{-1}.

Table S1. % yields calculated for solid complexes Ln.**1**$_3$ and Ln.**2**$_3$ (Ln = Tb^{III}, Sm^{III}, Lu^{III}, Dy^{III}) following preparation under microwave irradiation and isolation *via* diethyl ether diffusion.

Complex	Yield (%)	
	L = **1**	L = **2**
Tb.L_3	71	52
Sm.L_3	50	46
Lu.L_3	52	53
Dy.L_3	50	36

Table S2. Amide carbonyl stretching frequency shifts upon complexation of ligands **1** and **2** with 0.33 equiv. of $Ln(CF_3SO_3)_3$ (Ln = Tb^{III}, Sm^{III}, Lu^{III}, Dy^{III}).

Compound	Amide carbonyl stretching frequency (cm^{-1})	
	L = **1** (*R*) (1650 cm^{-1})	L = **2** (*S*) (1654 cm^{-1})
Tb.L_3	1634	1634
Sm.L_3	1633	1633
Lu.L_3	1635	1638
Dy.L_3	1634	1635

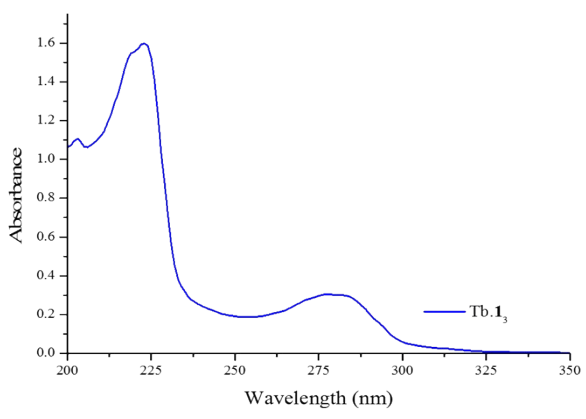

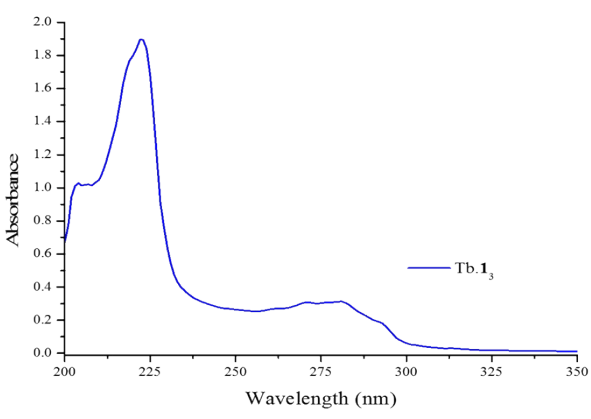

Figure S1. UV-Visible spectra of Tb.**1**$_3$ (*R*) recorded in (Left) CH_3CN (8.7 x 10^{-6} M) and (Right) CH_3OH (7.6 x 10^{-6} M).

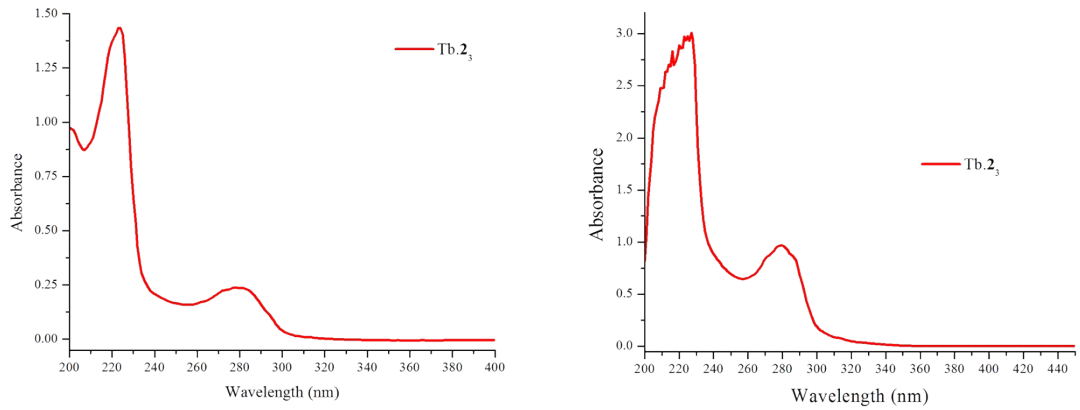

Figure S2. UV-Visible spectra of Tb.**2**$_3$ (*S*) recorded in (Left) CH_3CN (5.7 x 10^{-6} M) and (Right) CH_3OH (2.3 x 10^{-5} M).

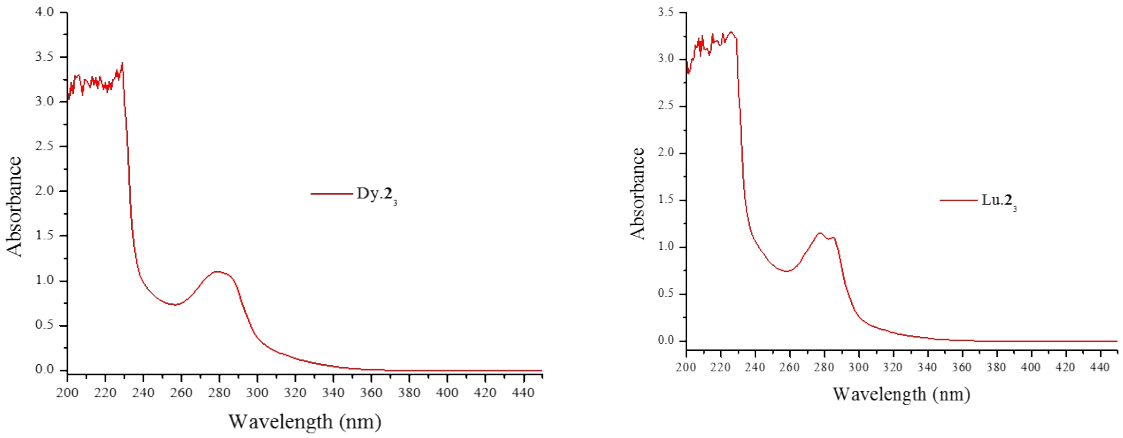

Figure S3 UV-visible absorption spectra of (Left) Dy.$\mathbf{2}_3$ (*S*) (3.1 x 10^{-5} M) and (Right) Lu.$\mathbf{2}_3$ (*S*) (2.9 x 10^{-5} M) in CH_3CN.

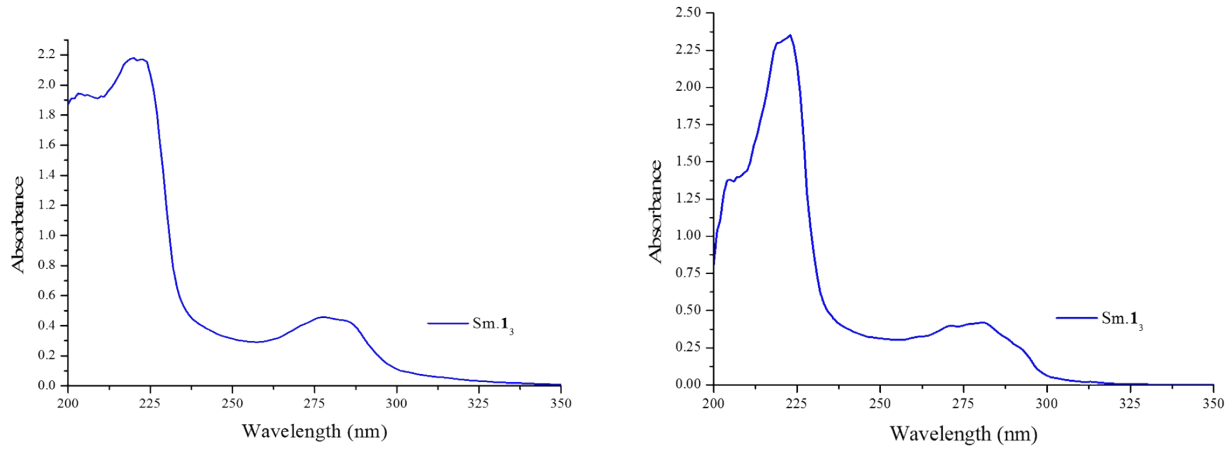

Figure S4. UV-Visible spectra of Sm.$\mathbf{1}_3$ (*R*) recorded in (Left) CH_3CN (1.2 x 10^{-5} M) and (Right) CH_3OH (1.1 x 10^{-5} M).

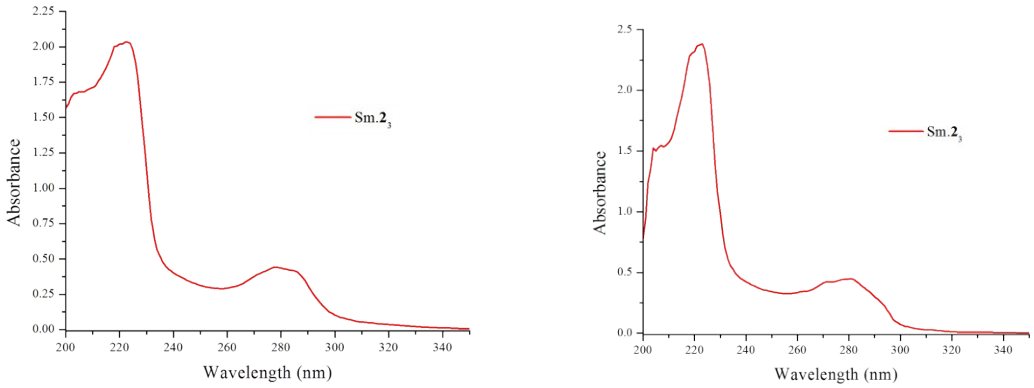

Figure S5. UV-Visible spectra of Sm.**2**$_3$ (*S*) recorded in (Left) CH_3CN (1.1 x 10^{-5} M) and (Right) CH_3OH (1.2 x 10^{-5} M).

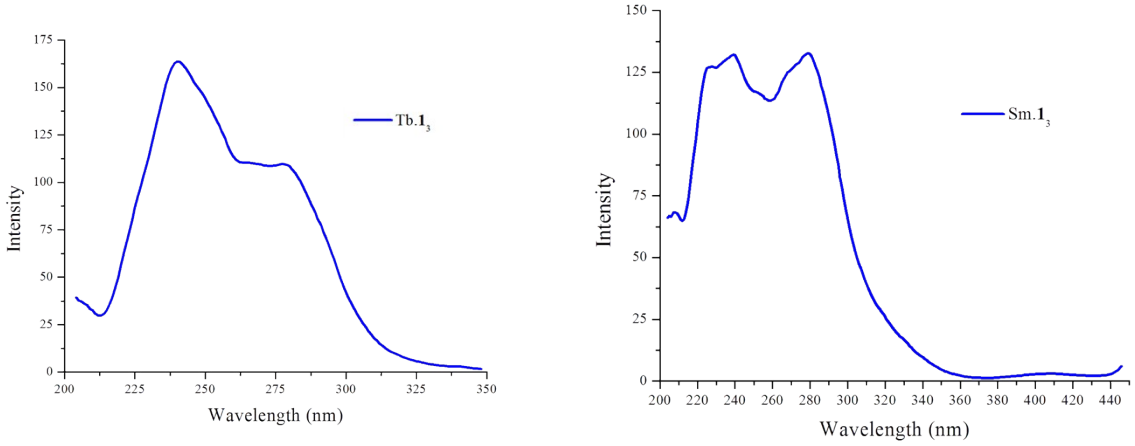

Figure S6. Excitation spectra of (Left) Tb.**1**$_3$ (*R*) (8.7 x 10^{-6} M) (λ_{em} = 545 nm) and (Right) Sm.**1**$_3$ (*R*) (1.2 x 10^{-5} M) (λ_{em} = 600 nm) recorded in CH_3CN.

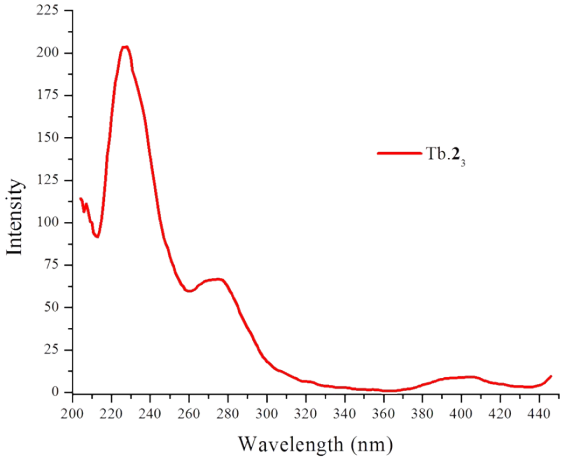

Figure S7. Excitation spectra of (Left) Tb.**2**$_3$ (*S*) (5.7 x 10^{-6} M) (λ_{em} = 545 nm)

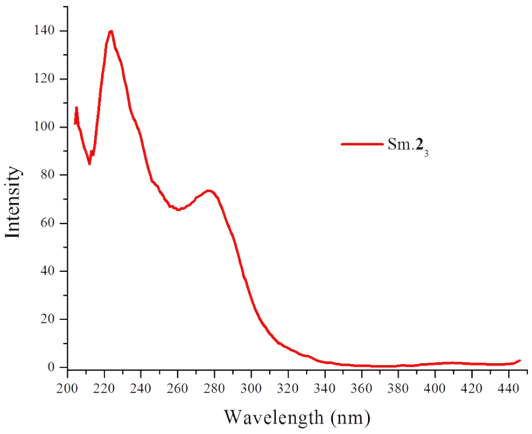

and (Right) Sm.$\mathbf{2}_3$ (*S*) (1.1 x 10^{-5} M) (λ_{em} = 600 nm) recorded in CH_3CN.

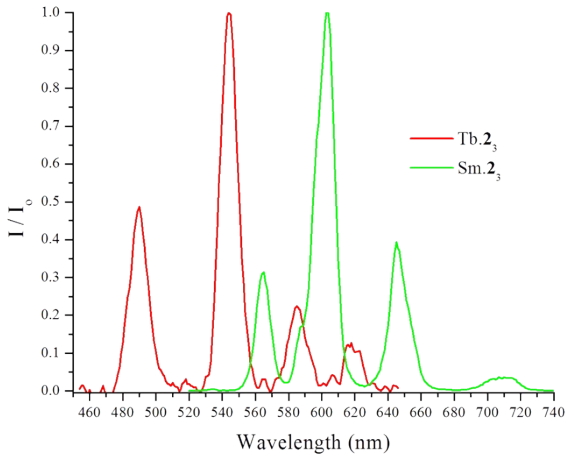

Figure S8. Normalised phosphorescence spectra of Tb.$\mathbf{2}_3$ and Sm.$\mathbf{2}_3$ recorded in CH_3CN.

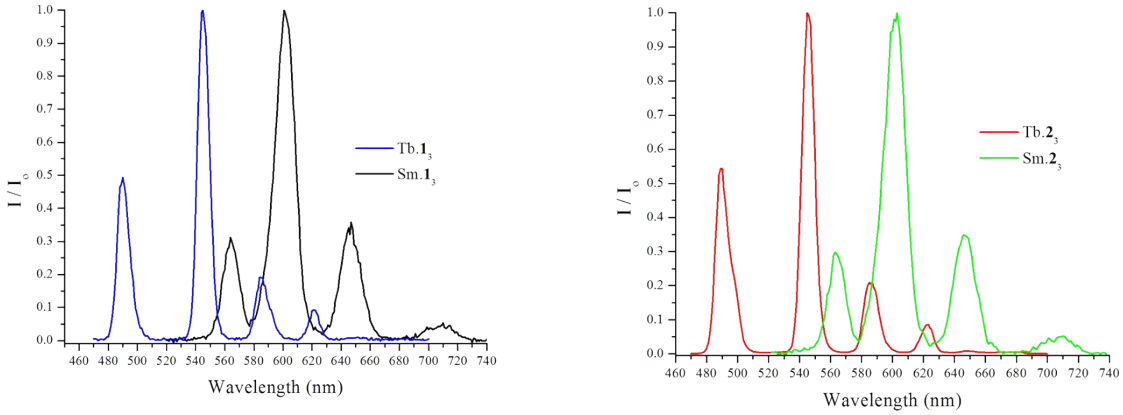

Figure S9. Normalised phosphorescence spectra of (Left) Tb.$\mathbf{1}_3$ (*R*) and Sm.$\mathbf{1}_3$ (*R*) and (Right) Tb.$\mathbf{2}_3$ (*S*) and Sm.$\mathbf{2}_3$ (*S*) recorded in CH_3OH.

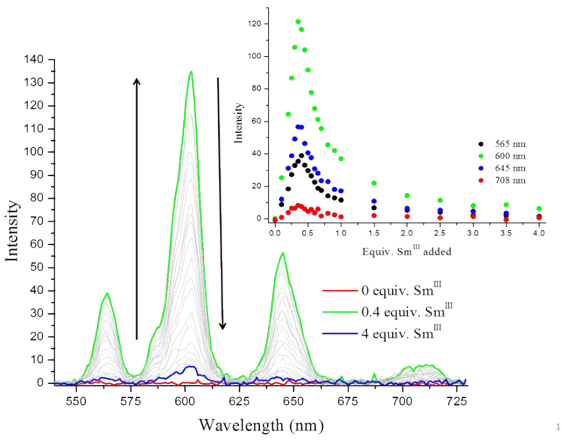

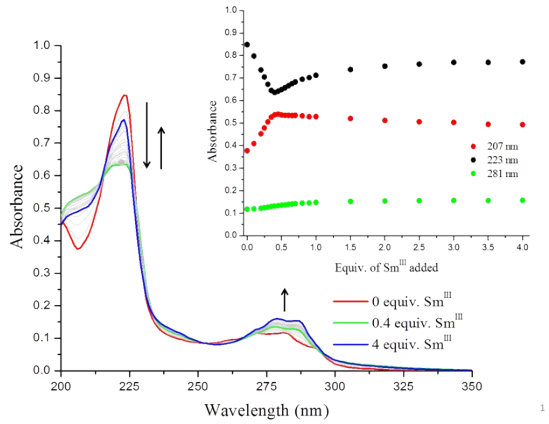

Figure S10. Overall changes in the (Left) UV-visible absorption spectra and (Right) Sm^{III}-centred phosphorescence spectra upon titrating of **1** (1 x 10^{-5} M) against $Sm(CF_3SO_3)_3$ (0→4 equiv.) in CH_3CN at RT. **Inset:** corresponding experimental binding isotherm of (Left) absorbance at λ = 207, 223 nm and 281 nm and (Right) Sm^{III} phosphorescence emission intensity at λ = 565 nm, 600 nm, 645 nm and 708 nm.

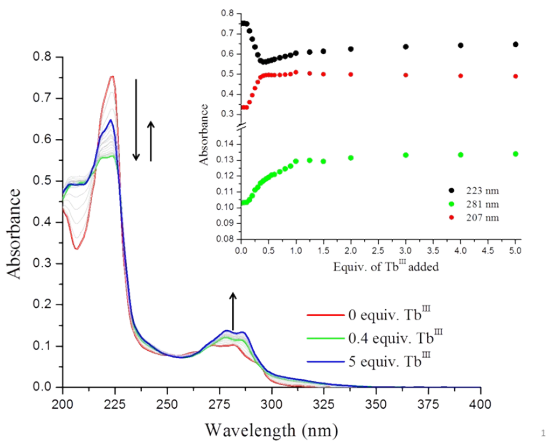

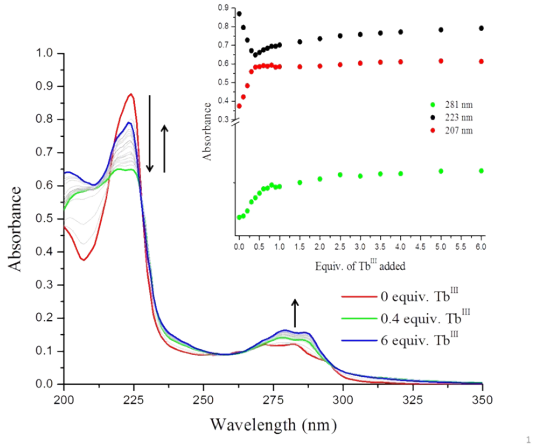

Figure S11. Overall changes in the UV-visible absorption spectra upon titrating (Left) **1** (0→5 equiv.) and (Right) **2** (0→6 equiv.) (1 x 10^{-5} M) against increasing $Tb(CF_3SO_3)_3$ in CH_3CN at RT. **Inset:** corresponding experimental binding isotherm of absorbance at λ = 207, 223 nm and 281 nm.

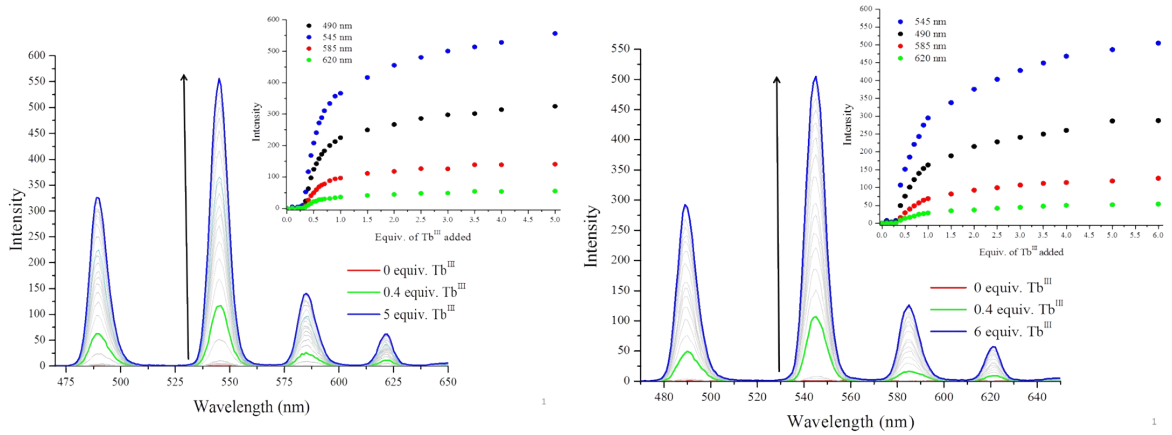

Figure S12. Overall changes in luminescence spectra upon titrating (Left) **1** (0→5equiv.) and (Right) **2** (0→6 equiv.) (1 x 10^{-5} M) against $Tb(CF_3SO_3)_3$ in CH_3CN at RT. **Inset:** corresponding experimental binding isotherm of luminescence at λ = 490, 545, 585 and 620 nm.

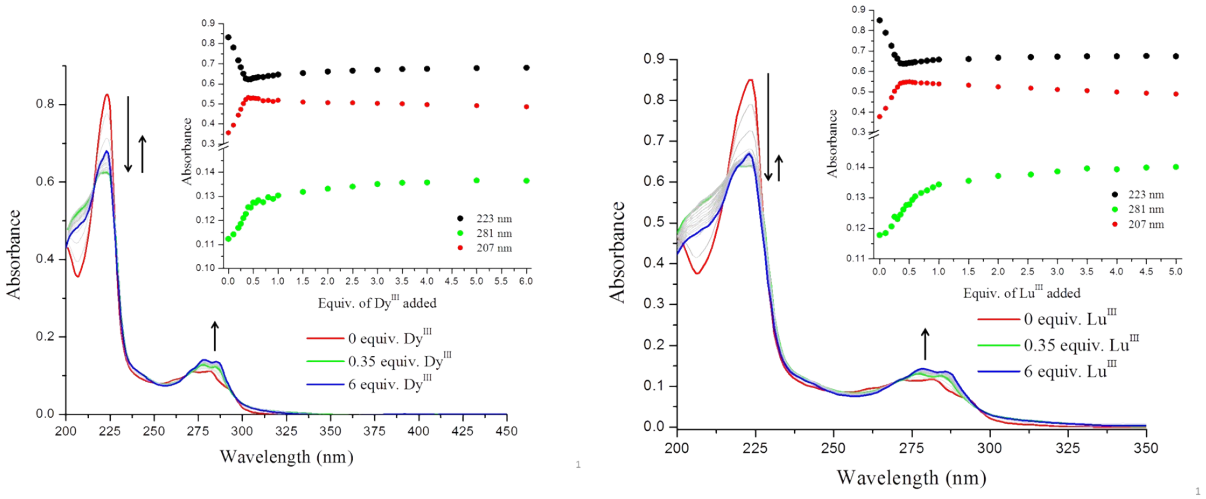

Figure S13. Overall changes in the UV-visible absorption spectra upon titrating **1** (1 x 10^{-5} M) against (Left) $Dy(CF_3SO_3)_3$ (0→6 equiv.) and (Right) $Lu(CF_3SO_3)_3$ (0→5 equiv.) in CH_3CN at RT. **Inset:** corresponding experimental binding isotherm of absorbance at λ = 207, 223 nm and 281 nm.

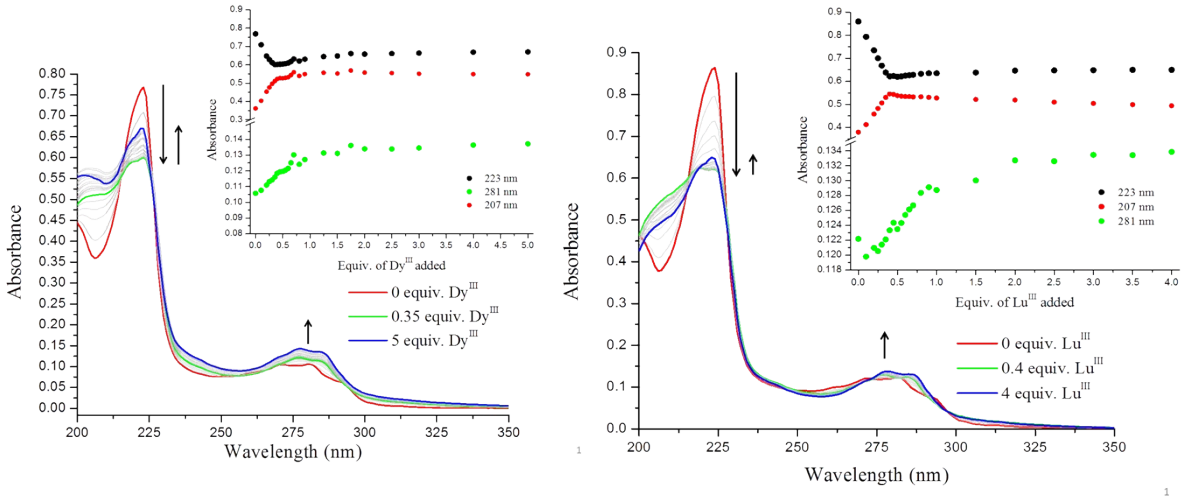

Figure S14. Overall changes in the UV-visible absorption spectra upon titrating **2** (1 x 10^{-5} M) against (Left) $Dy(CF_3SO_3)_3$ (0→5 equiv.) and (Right) $Lu(CF_3SO_3)_3$ (0→4equiv.) in CH_3CN at RT. **Inset:** corresponding experimental binding isotherm of absorbance at λ = 207, 223 nm and 281 nm.

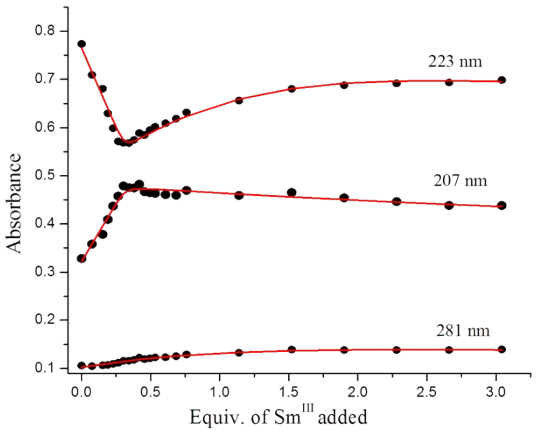

Figure S15. Fit of the experimental binding isotherms using the non-linear regression analysis program SPECFIT (upon titrating **2** against $Sm(CF_3SO_3)_3$ in CH_3CN).

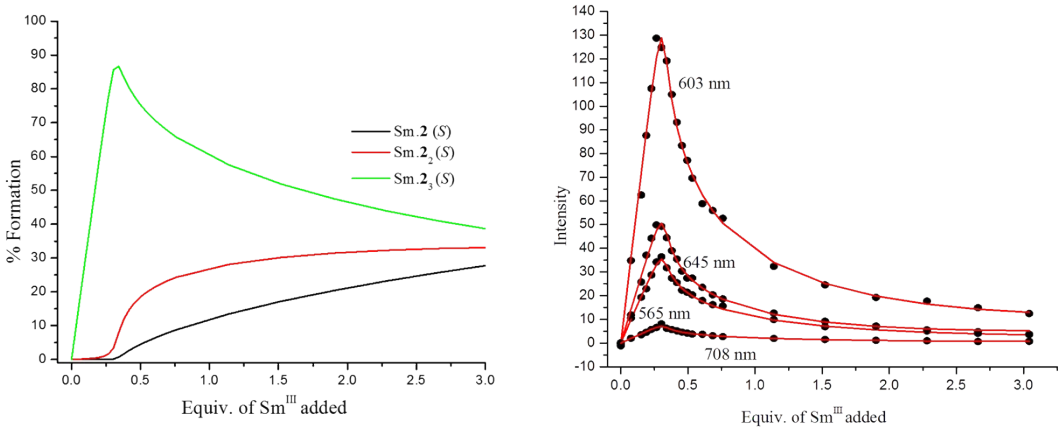

Figure S16. (Left) The speciation distribution diagram obtained from the luminescence titration data fit (upon titrating **2** against $Sm(CF_3SO_3)_3$ in CH_3CN) and (Right) the fit of the experimental binding isotherms using the non-linear regression analysis program SPECFIT.

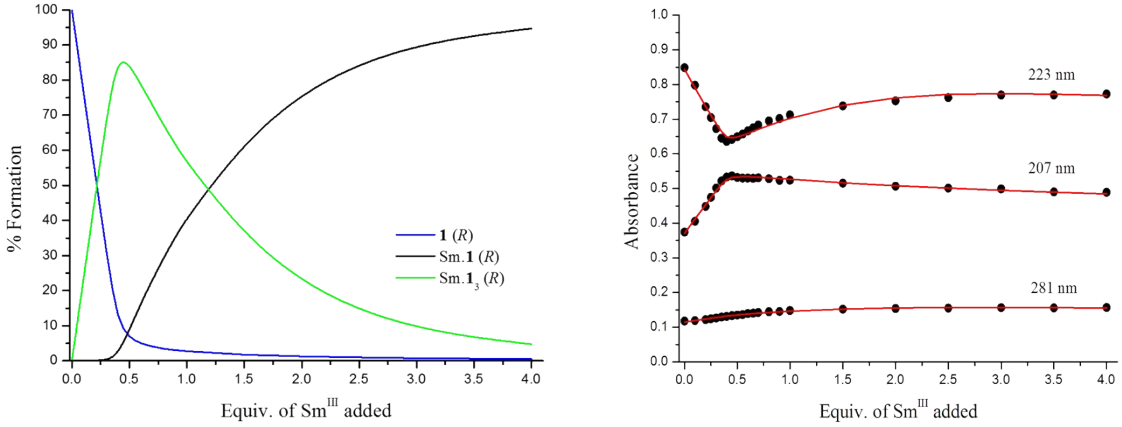

Figure S17. (Left) The speciation distribution diagram obtained from the UV-visible absorption titration data fit (upon titrating ligand **1** against $Sm(CF_3SO_3)_3$ in CH_3CN) and (Right) the fit of the experimental binding isotherms using the non-linear regression analysis program SPECFIT.

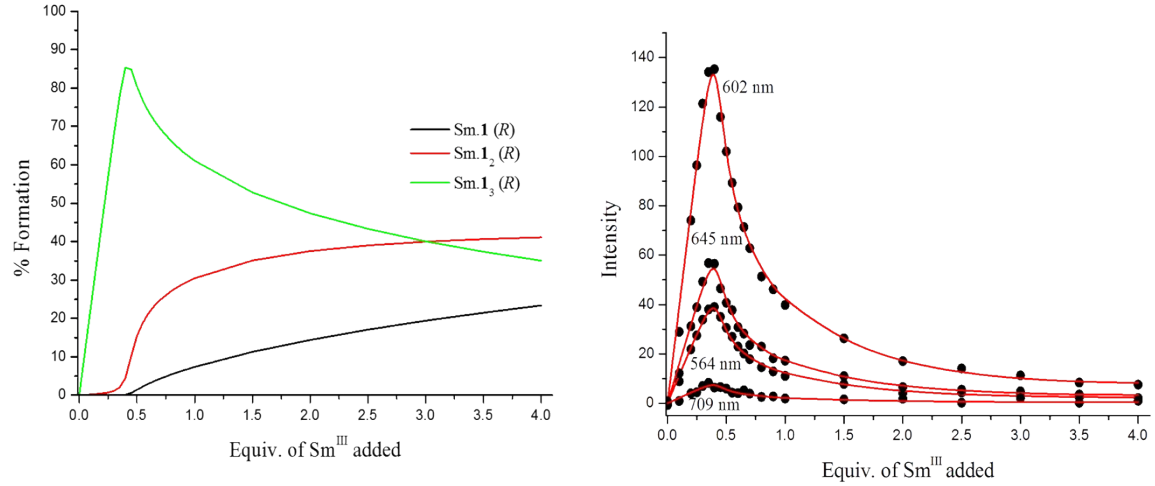

Figure S18. (Left) The speciation distribution diagram obtained from the luminescence titration data fit (upon titrating ligand **1** against $Sm(CF_3SO_3)_3$ in CH_3CN) and (Right) the fit of the experimental binding isotherms using the non-linear regression analysis program SPECFIT.

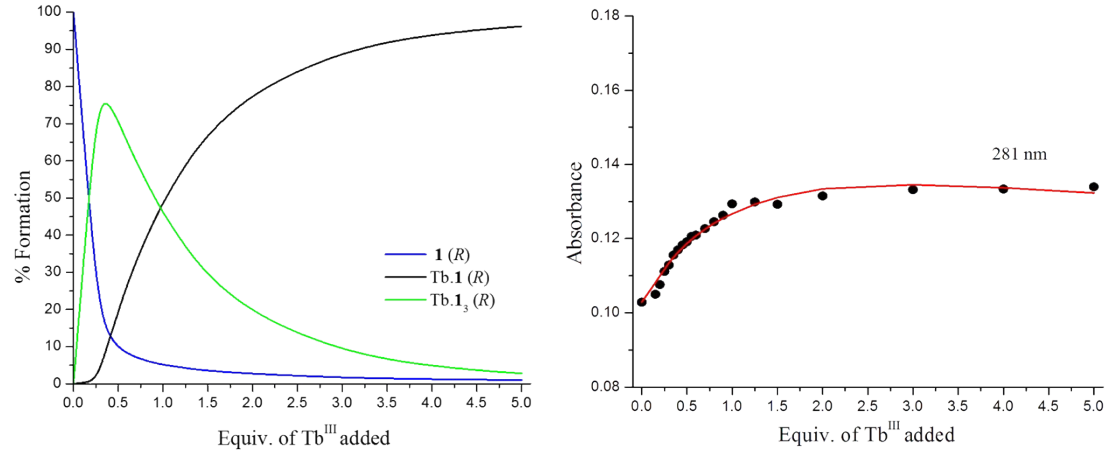

Figure S19. (Left) The speciation distribution diagram obtained from the UV-visible absorption titration data fit (upon titrating ligand **1** against $Tb(CF_3SO_3)_3$ in CH_3CN) and (Right) the fit of the experimental binding isotherms using the non-linear regression analysis program SPECFIT.

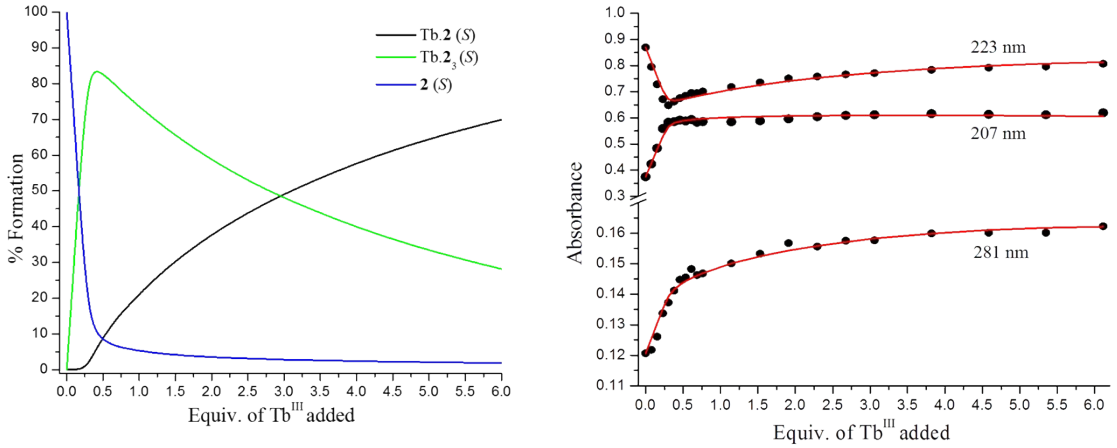

Figure S20. (Left The speciation distribution diagram obtained from the UV-visible absorption titration data fit (upon titrating ligand **2** against $Tb(CF_3SO_3)_3$ in CH_3CN) and (Right) the fit of the experimental binding isotherms using the non-linear regression analysis program SPECFIT.

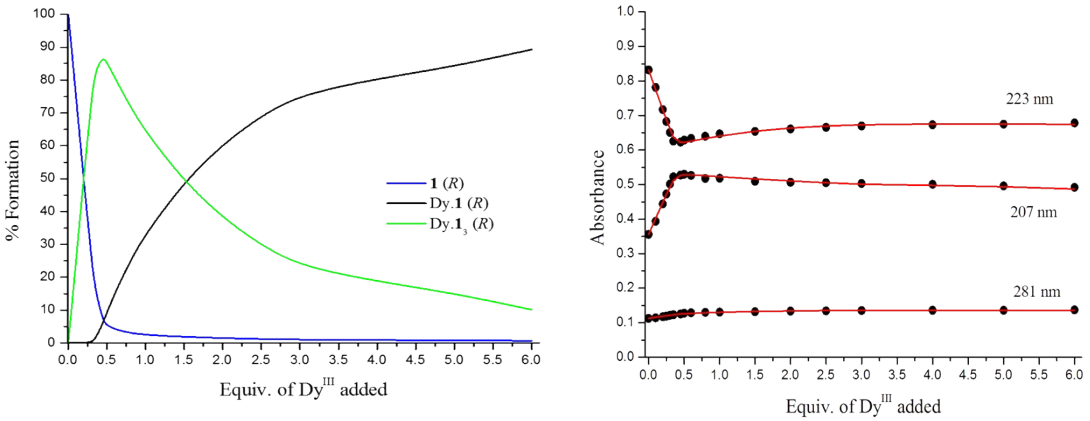

Figure S21. (Left) The speciation distribution diagram obtained from the UV-visible absorption titration data fit (upon titrating ligand **1** against $Dy(CF_3SO_3)_3$ in CH_3CN) and (Right) the fit of the experimental binding isotherms using the non-linear regression analysis program SPECFIT.

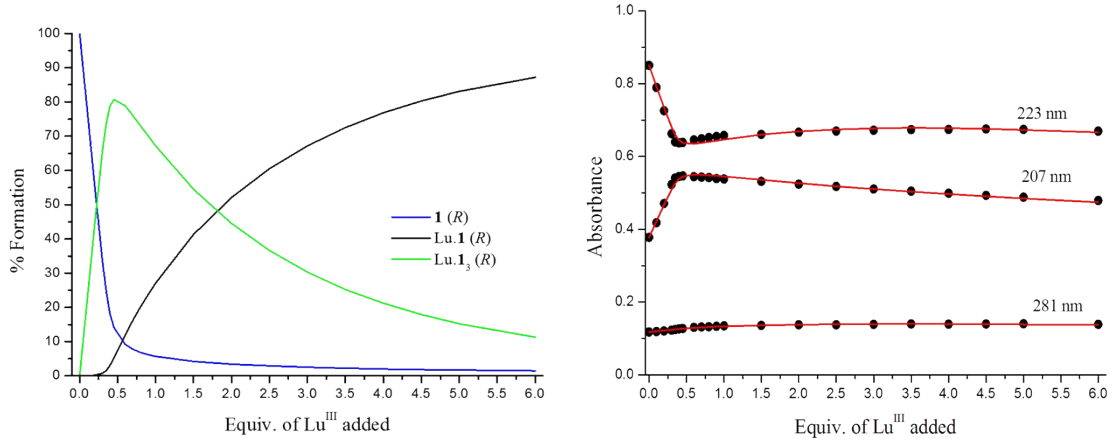

Figure S22. (Left) The speciation distribution diagram obtained from the UV-visible absorption titration data fit (upon titrating ligand **1** against $Lu(CF_3SO_3)_3$ in CH_3CN) and (Right) the fit of the experimental binding isotherms using the non-linear regression analysis program SPECFIT.

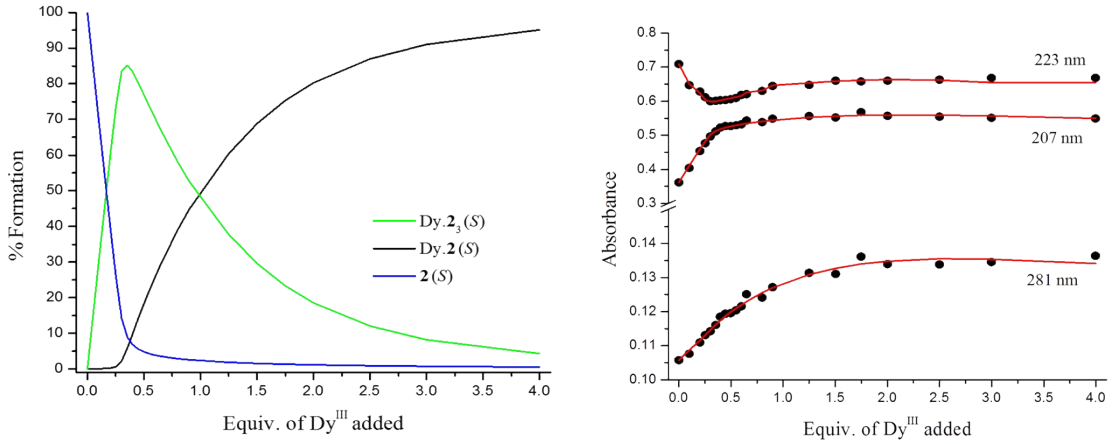

Figure S23. (Left) The speciation distribution diagram obtained from the UV-visible absorption titration data fit (upon titrating ligand **2** against $Dy(CF_3SO_3)_3$ in CH_3CN) and (Right) the fit of the experimental binding isotherms using the non-linear regression analysis program SPECFIT.

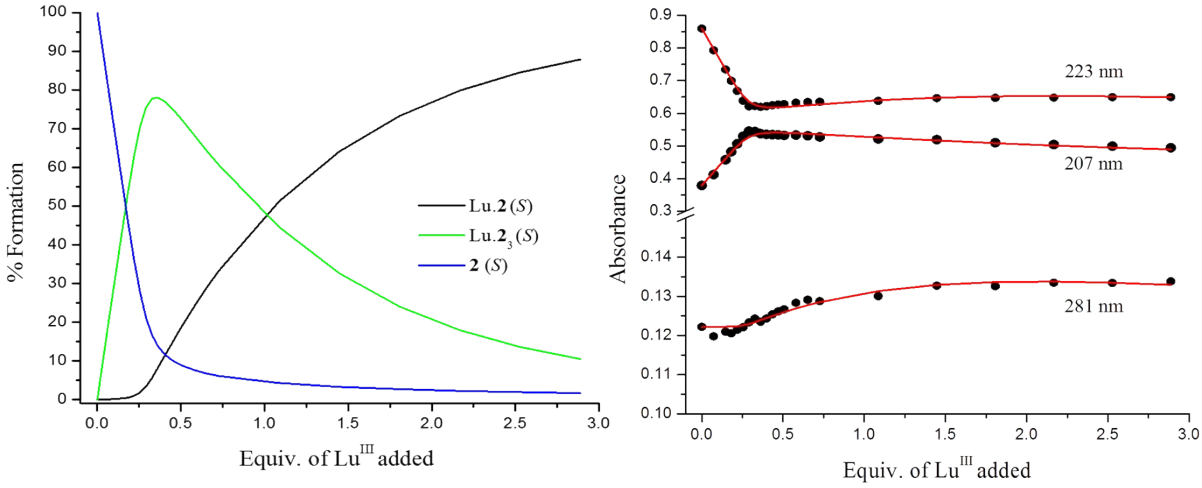

Figure S24. (Left) The speciation distribution diagram obtained from the UV-visible absorption titration data fit (upon titrating ligand **2** against $Lu(CF_3SO_3)_3$ in CH_3CN) and (Right) the fit of the experimental binding isotherms using the non-linear regression analysis program SPECFIT.

Table S3. Summary of binding constants obtained from non-linear regression analyses of data from ligands **1** (top) and **2** (bottom) titrated against $Ln(CF_3SO_3)_3$ (Ln = Tb, Sm, Lu, Dy).

$Ln.L_3$	UV-visible absorption		Luminescence		
	$\log \beta_{11}$	$\log \beta_{13}$	$\log \beta_{11}$	$\log \beta_{12}$	$\log \beta_{13}$
$Tb.\mathbf{1}_3$	6.4*	18.3 ± 0.2	-	-	-
$Sm.\mathbf{1}_3$	6.8 ± 0.2	19.4 ± 0.4	6.2 ±0.2	13.4 ± 0.1	20.4 ± .2
$Dy.\mathbf{1}_3$	6.6 ± 0.2	19.4 ± 0.4	-	-	-
$Lu.\mathbf{1}_3$	6.2 ± 0.2	18.3 ± 0.3	-	-	-
$Tb.\mathbf{2}_3$	5.8 ± 0.2	18.1 ± 0.3	-	-	-
$Sm.\mathbf{2}_3$	6.8± 0.2	19.8 ± 0.5	6.2 ± 0.2	13.2 ± 0.2	20.3 ± 0.2
$Dy.\mathbf{2}_3$	6.7 ± 0.2	19.4 ± 0.4	-	-	-
$Lu.\mathbf{2}_3$	6.3 ± 0.2	18.3 ± 0.3	-	-	-

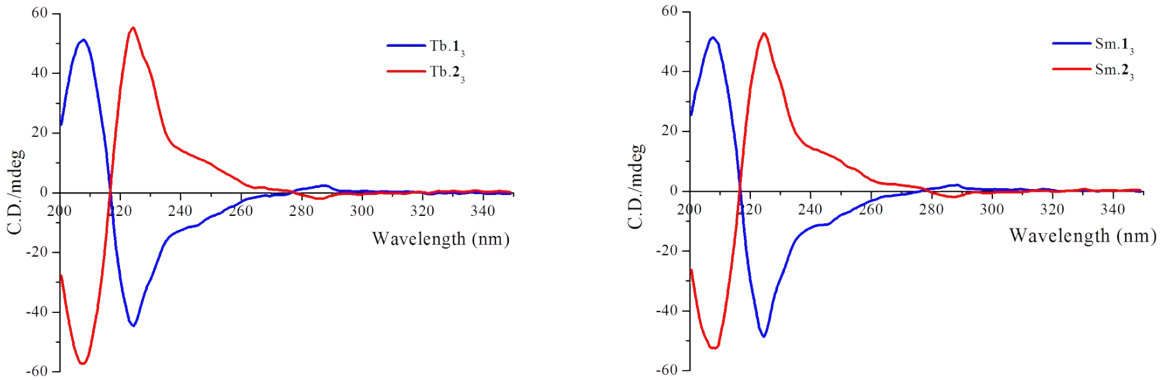

Figure S25. The circular dichroism spectra of **1** and **2** (2 x 10^{-5} M) recorded in CH_3CN at RT after the addition of 0.33 equiv. of (Left) $Tb(CF_3SO_3)_3$ and (Right) $Sm(CF_3SO_3)_3$ - note that discrepancies in intensities can be derived from the slight differences in concentrations.

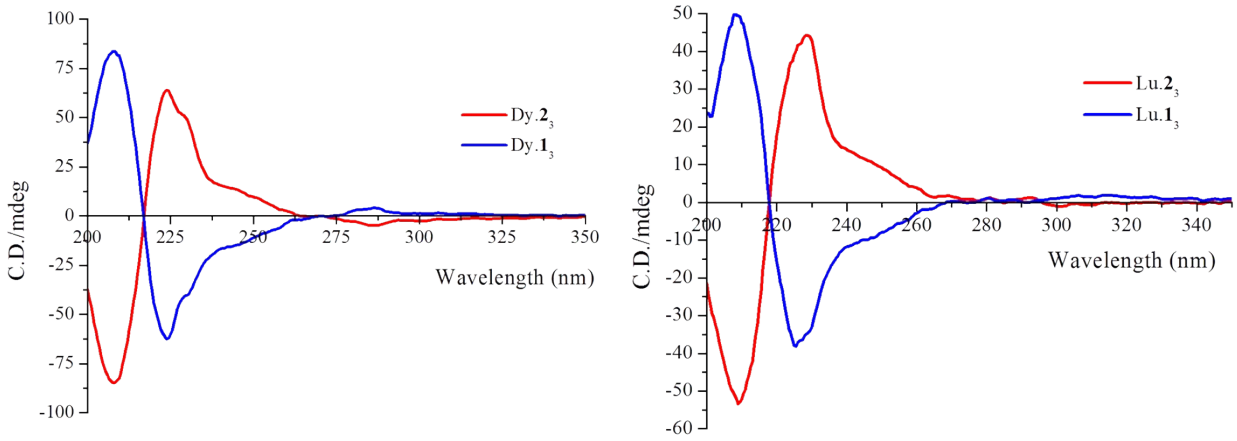

Figure S26. The circular dichroism spectra of **1** (3.9 x 10^{-5} M) and **2** (3.3x 10^{-5} M) recorded in CH_3CN at RT after the addition of 0.33 equiv. of (Left) $Dy(CF_3SO_3)_3$ and (Right) $Lu(CF_3SO_3)_3$ - note that discrepancies in intensities can be derived from the slight differences in concentrations.

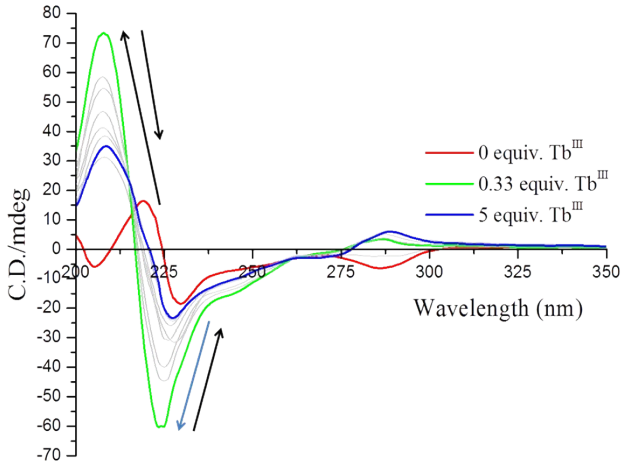

Figure S27. The overall changes in the CD spectra of **1** (*R*) (3.5 x 10^{-5} M) upon titrating against increasing concentrations of $Tb(CF_3SO_3)_3$ (0→5 equiv.) at RT in CH_3CN.

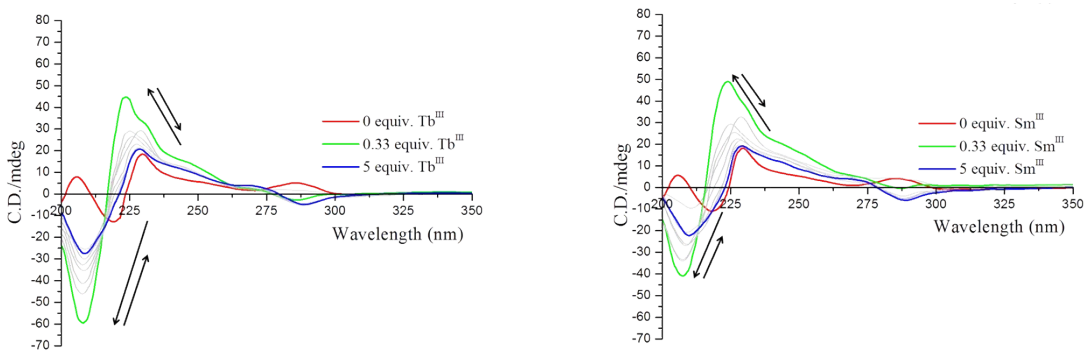

Figure S28. The overall changes in the CD spectra of **2** (*S*) (3.4 x 10^{-5} M for (Left) and 3.3 x 10^{-5} M for (Right)) upon titrating against increasing concentrations of (Left) $Tb(CF_3SO_3)_3$ (0→5 equiv.) and (Right) $Sm(CF_3SO_3)_3$ (0 – 5 equiv.) at RT in CH_3CN.

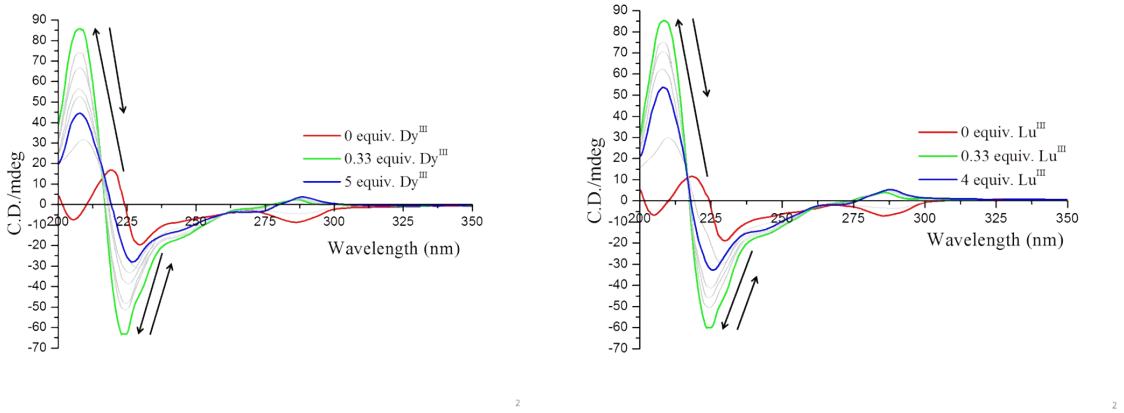

Figure S29. The overall changes in the CD spectra of **1** (*R*) (3.6 x 10^{-5} M for (Left) and (3.5 x 10^{-5} M) for (Right)) upon titrating against increasing concentrations of (Left) $Dy(CF_3SO_3)_3$ (0→5 equiv.) and (Right) $Lu(CF_3SO_3)_3$ (0→4 equiv.) at RT in CH_3CN.

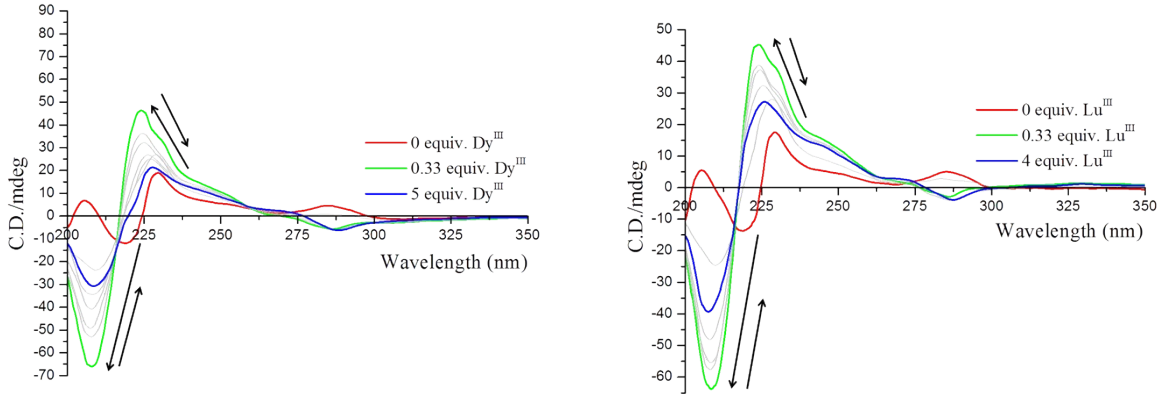

Figure S30. The overall changes in the CD spectra of **2** (*S*) (3.4 x 10^{-5} M for (Left) and (3.4 x 10^{-5} M) for (Right)) upon titrating against increasing concentrations of (Left) $Dy(CF_3SO_3)_3$ (0→5 equiv.) and (Right) $Lu(CF_3SO_3)_3$ (0→4 equiv.) at RT in CH_3CN.

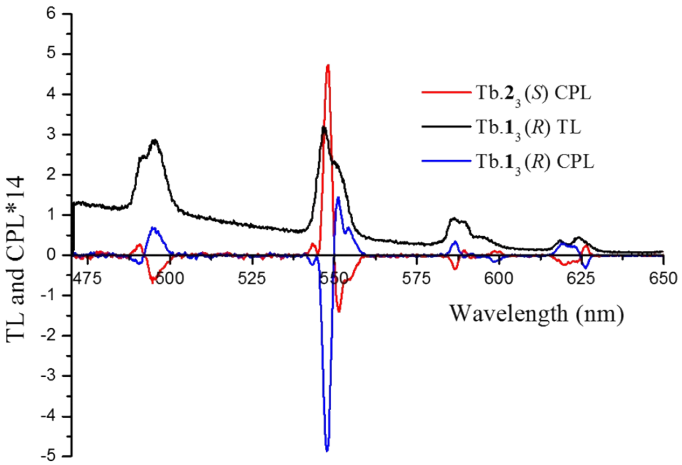

Figure S31. Total Ln^{III}-centred emission and CPL spectra of complexes Tb. $\mathbf{1}_3$ (*R*) and Tb.$\mathbf{2}_3$ (*S*) recorded in CH_3CN (excitation at λ = 281nm).

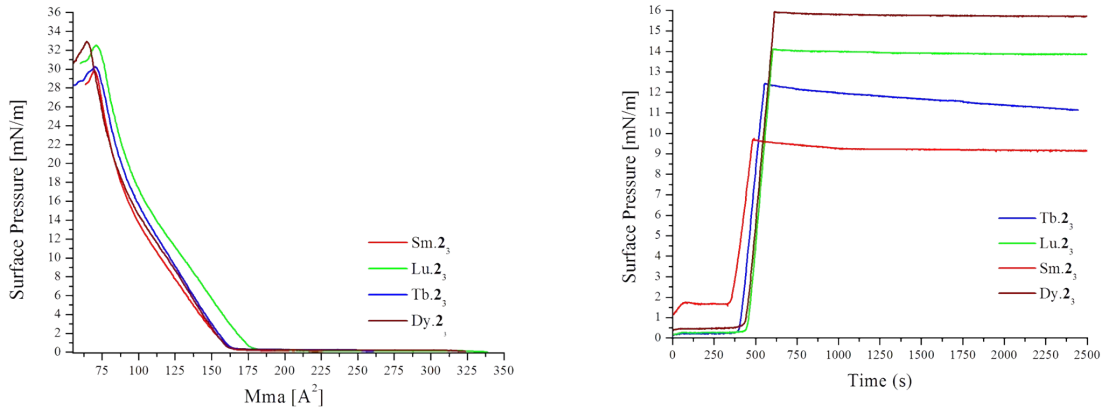

Figure S32. (Left) Surface pressure-area isotherm of Ln.$\mathbf{2}_3$ and (Right) monolayer stability graph of Ln.$\mathbf{2}_3$.

Table S4. Surface-pressure and corresponding mean molecular area values upon film collapse for Ln.$\mathbf{L}_3$ (Ln = Eu^{III}, Nd^{III}, Tb^{III}, Sm^{III}, Lu^{III}, Dy^{III} and L = **1** and **2**). *Data from references 21(a) and 22.

Complex	Surface-pressure at collapse (mN/m)		Mean molecular area (A^2/molecule)	
	L = **1**	L = **2**	L = **1**	L = **2**
Eu.$\mathbf{L}_3^*$	34	29	74	76
Nd.$\mathbf{L}_3^*$	32	33	71	74
Tb.$\mathbf{L}_3$	33	30	66	71
Sm.$\mathbf{L}_3$	35	30	70	70
Lu.$\mathbf{L}_3$	34	33	62	71
Dy.$\mathbf{L}_3$	32	33	58	65

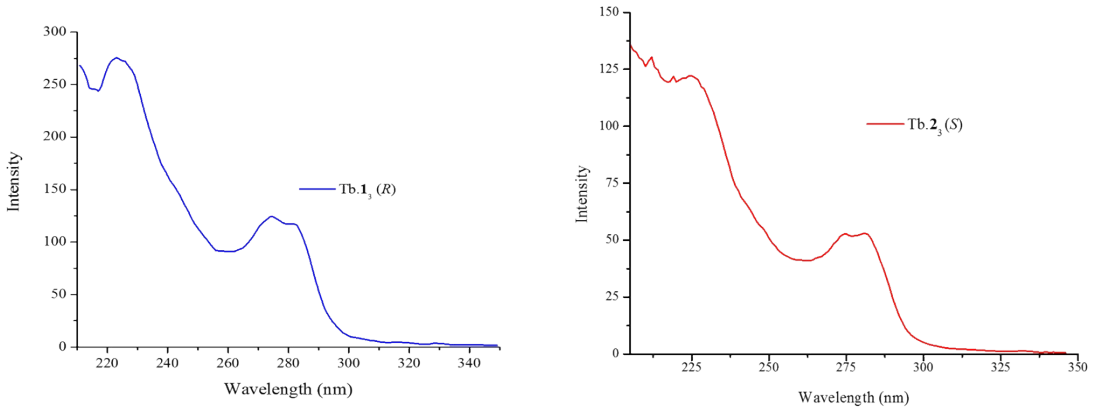

Figure S33. Excitation spectra (λ_{em} = 545 nm) of (Left) Tb.$\mathbf{1}_3$ and (Right) Tb.$\mathbf{2}_3$ LB monolayers.